

# Self Healing Concrete – A Sustainable Future

---

Simon Dunn, BEng (hons), Cardiff University

## Abstract

The cement industry is a major global contributor to world CO<sub>2</sub> emissions (8% in 2008). A major cause of this high percentage is the durability issues associated with concrete. In recent years a new breed of concrete that has the ability to heal cracks which are a major cause of these durability issues has been developed called Self-healing Concrete. This paper will introduce this new breed of concrete in its various forms, with particular attention paid to the form which incorporates shape memory polymers as the healing mechanism. The shape memory polymer-cementitious composite has been developed at Cardiff University and is the subject of a patent pending. The paper will focus on the experimental and numerical work undertaken to understand the material behaviour of shape memory polymers and how this can be applied to the cementitious composite. A numerical model has been developed and the successful comparison to experimental data will be presented.

## 1. Introduction

The environmental impact of the cement industry is an ever increasing concern for engineers, with the cement industry generating approximately 8% of all the world CO<sub>2</sub> emissions (2008 figures) (1) up from 5% in 2001 (2). When compared to the aviation industry which contributes 2% of world CO<sub>2</sub> emissions (3), it is clear as engineers we have a major part to play in protecting future generations from global warming. In addition to the environmental impact of the cement industry, the economic impact is also a major issue. Approximately half of the £80x10<sup>9</sup> spent on construction work in the UK per annum is allocated to repair and maintenance of existing structures, many of which are concrete structures (4). A more durable cementitious material will allow less maintenance and a longer working life, reducing the amount of cement required and thus the environmental and economic impact.

The durability of concrete is compromised by the ingress of harmful chemicals such as saline water, CO<sub>2</sub> and acid rain into cracks created during early age shrinkage and/or mechanical loading. The current practice is to overdesign the structure in order to achieve a maximum crack width between 0.1 and 0.4mm under long term serviceability loading (5). A commonly used solution is to make use of pre-stress by pre or post-tensioning. These pre-stressed structures are designed to be uncracked during serviceability loading, although in recent times there have been problems with the durability of such structures. The major problem with the pre-stressed system is that steel tendons are relatively expensive and require expensive anchors and jacking operations, which themselves also pose a health and safety issue.

There have been many recent developments in the production of more durable concrete, namely that of self-healing concrete. Despite its relative infancy, it provides a valid and practical solution to the problem.

This paper will introduce self-healing concrete in its various forms and particular attention will be paid to the solution being developed at Cardiff University which utilises shape memory polymers (6). The main focus of this paper will be the determination and subsequent numerical simulation of a suitable shape memory polymer. Experimental data and comparisons with numerical data will be presented. The main aims of this research have been to:

- (1) Determine a suitable shape memory polymer,
- (2) Understand the behaviour of the chosen material,
- (3) Produce a successful numerical model, validated by experimental data.

## **2. Self Healing of Cementitious Composites**

The development of self-healing cementitious composites is a relatively new area of research which to this date has focused both on the natural ability of hydrates to heal cracks over time (autogenic) and artificial means of crack repair that are man-made inclusions (autonomic) (7). The motivation for such work is to increase the durability of concrete.

The natural self healing ability of concrete, known as autogenous healing, has been understood for around 20 years (8). The effect can be seen in many old structures which have survived for such long periods of time with only limited maintenance. Cracks in old concrete structures such as Roman aqueducts and gothic churches have been seen to heal when moisture interacts with unhydrated cement clinker in the crack. However in recent structures the cement content is reduced due to modern construction methods and hence the amount of available unhydrated cement is lower (9) and the natural healing effect is reduced. The three main processes of autogenous healing according to Joseph (10) are (i) swelling and hydration of cement pastes; (ii) precipitation of calcium carbonate crystals, and; (iii) blockage of flow paths due to deposition of water impurities or movement of concrete fragments that detach during the cracking process. Numerous authors in recent years have investigated various situations that affect the amount and rate of autogenic healing including the effect of temperature (11), degree of damage (12), freeze-thaw cycles (13) and the age of the concrete (14). The mix composition of the mortar can also be used to enhance the autogenic behaviour, for example by including blast furnace slag into the mix (9). It was found that maximum healing occurred in early age concrete (15) and specimens tested under water showed the best strength recovery, hence it was concluded that the primary healing mechanism was ongoing hydration.

The man-made self healing ability of concrete, known as autonomic healing was first introduced by Dry in 1994 (16). The system proposed by Dry was similar to that used in polymers in which a healing agent is encapsulated inside a microcapsule and when a crack forms it breaks the microcapsule, releasing the healing agent and healing the crack. There are two main aspects to consider with regard to the autonomic healing concept, namely, the encapsulation method and the healing agent that is encapsulated.

There have been a number of healing agents proposed, however these are generally 'off the shelf' agents, making them relatively low cost and readily available. This suits the nature of their use in large bulk material such as concrete (10). To date the most common healing agents proposed are epoxy resins, cyanacrylates, and alkali-silica solutions. Joseph states that there are a number of

pre-requisites that an agent must possess including, a suitably low viscosity to ensure a wider repair area and a sufficiently strong bond between crack surfaces and that there should be adequate capillary forces to draw the agent into the crack. A system developed by Nishiwaki et al (17) stores a low viscosity epoxy resin in an organic film pipe that melts at 93°C. Upon formation of a crack, sensed via a strain gauge, there is a reduction in electrical conductivity and hence increased resistance and temperature. This increased temperature melts the organic supply tube and cures the epoxy resin after it has flowed into the crack. Cyanoacrylates, commonly known as super glues, are one part systems that in the presence of moisture react and cure very rapidly forming a bond often stronger than the material it is bonding, i.e. concrete. Hence the healed crack is actually stronger than the surrounding material itself. This system has been rigorously tested and developed by Joseph (10) who showed that if a system is damaged and healed and then damaged again, a new crack will form around the healed crack. The use of cyanoacrylates in concrete is further enhanced by them being an acidic solution which due to the concrete's alkaline environment causes yet quicker healing. Finally, alkali-silica solutions have also been utilized as healing agents mainly by Mihashi et al. (18) who state that in the presence of oxygen the solution causes hydration and hence bonding of the original crack faces. Although this system produces a lower bond strength, it causes less material compatibility problems than the previous two systems.

The previously described healing agents require a method to encapsulate them in the cementitious matrix until they are required for healing. Several methods have been proposed including the use of micro-capsules, a continuous glass supply tube (18) and capillary tubes (19) which are embedded in the concrete. Microcapsules have the advantage that the concrete can react to diffused cracking in multiple locations, although once a capsule has "been utilized" it cannot be refilled and it remains a void in the concrete. Capillary tubes used in the medical profession for blood testing have been embedded in concrete as encapsulating vessels for ethyl cyanoacrylate healing agent. Experiments showed that despite some localized debonding between the tube and cement matrix, the system was successful in sensing crack propagation and actuating accordingly healing the crack (19). Finally, continuous glass supply pipes which have the advantage of being able to vary the healing agent and supply additional healing agent have proven successful in healing larger fractures (18). The issue with such a system however is that care must be taken in placing the glass tubes and hence is not suitable for cast in-situ concrete.

One further and very interesting method of producing self-healing concrete is being developed at DELFT University in The Netherlands which makes use of mineral producing bacteria. In this system the bacteria act as a catalyst and transform a precursor compound into a suitable filler material, such as calcium carbonate based mineral precipitates. The filler material then acts as a type of bio-cement which effectively seals newly formed cracks (20).

The proposed system being developed at Cardiff University combines both the autogenic healing and autonomic principles in that it makes use of a man-made system to enhance the natural autogenic healing and repair cracks in concrete. The system incorporates shape memory polymers into the cementitious matrix to place the crack in the most favourable conditions for autogenous healing to occur.

### 3. Proposed Cementitious-Shape Memory Polymer Composite

The proposed cementitious-shape memory polymer composite system being developed at Cardiff University is the subject of a previous paper (21) and has a patent pending (22). The aim of the system is to improve the durability of cementitious materials by incorporating a mechanism for crack closure into the cementitious matrix. The self repairing of cracks will prevent the ingress of harmful chemicals such as saline water, acid rain and CO<sub>2</sub>, all of which reduce the working life of concrete structures.

Shape memory polymers are semi-crystalline polymers which have a predefined shape memorised in their material structure. In the case of the proposed system the memorised state is a shorter specimen than the current material, so that upon activation the specimen will contract or shrink and in a restrained condition generate a shrinkage force (23).

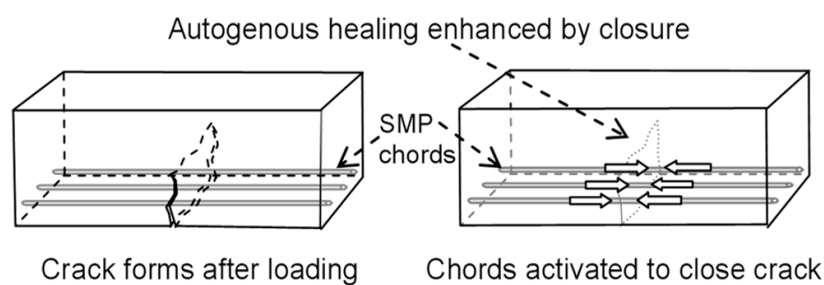


*Figure 1: Proposed shape-memory polymer-cementitious composite*

Upon crack formation the system seen in Figure 1 will be triggered. The shape memory polymer, which is anchored within a cavity in the cementitious matrix is activated via heating. Heating can be in the form of direct heat or electrical current via an increase in temperature due to high ohmic resistance. Upon activation the shape memory effect or shrinkage occurs and due to the restrained nature of the tendon, a tensile force is generated. This tensile force in turn imparts a compressive force to the cementitious matrix at the crack location and hence the crack closes. Autogenous healing then occurs and is enhanced by the crack being put into this compressive state (15). Studies into further enhancing this autogenous healing have also been carried out and this is the subject of a forthcoming publication (24).

#### 3.1. Material Screening Study

In order to determine a suitable material for the proposed system a pilot study was undertaken (25). The suitable material must be capable of developing a shrinkage stress of 20MPa following activation in a restrained condition. The activation may be initiated by heat applied directly or via an electrical current. The temperature of stress development must occur between 70-90°C to prevent premature activation during the hydration process of the cementitious material or damage to surrounding concrete. Future considerations include that the material should also be inert to alkaline environment and maintain >70% of the shrinkage stress for the working life of the structure (6). The screening tests highlighted Aerovac Shrinktite, a drawn polyethylene terephthalate (PET) polymer material, manufactured in 32x0.046mm tapes as best suiting the criteria.

### 3.2. Experimental Simulation of Shape Memory Polymer

A series of experiments were carried out on the chosen PET material to determine both the material properties and shrinkage effects with temperature. Reference (26) provides a detailed summary of further experimental work.

#### 3.2.1. Specimen Preparation and Testing Procedure

Specimen preparation was required to enable a suitable and accurate test procedure. The testing procedure and preparation was the result of a series of preliminary investigations to ensure an accurate and reliable data set. In order to minimise slippage of the specimens when gripped the PET tapes were manufactured into a collection of 25 strips each measuring 6mm x 0.046mm x 450mm in length, bonded at either end using a soldering iron and specially designed jig (26). Two steel plates (10x20x3mm) were then placed at a distance of 360mm apart and centrally on the specimen. The remaining length of polymer was then melted to create a mechanical plug, which serves as a mechanical lock preventing slippage, as seen in Figure 2(b).

The specimens were then loaded into grips in a Dartec tensile testing machine fitted with an Instron environmental chamber capable of temperatures ranging from -50°C to +250°C as seen in Figure 2(a). A pre-load of 50N was applied to remove any slack.

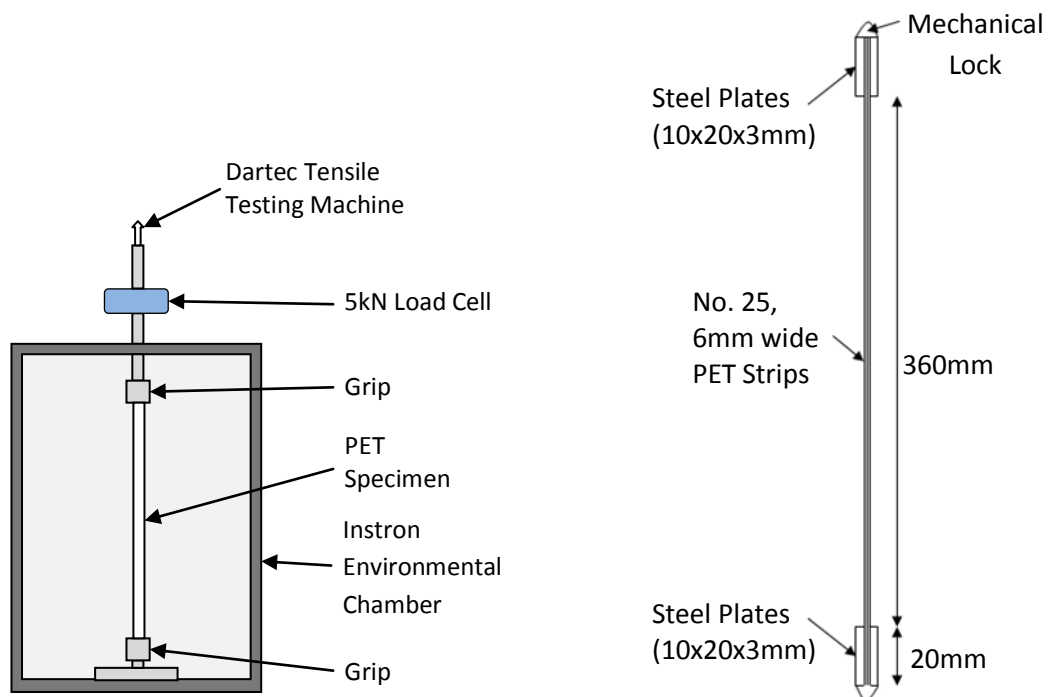


Figure 2: Experimental Set-up, (a) Thermal Chamber and (b) Specimen

Two parametric studies were then undertaken to investigate the development of shrinkage with temperature and the development of the Young's modulus with temperature.

#### 3.2.2. Development of Shrinkage Stress with Temperature

The specimen was held at constant displacement while the stress, time and temperature was monitored as the temperature was raised rapidly to 90°C and soaked for 3 hours before returning

the temperature to ambient and soaking for a further 1 hour. Plots of stress development with both temperature and time were achieved and can be seen in Figures 3a and 3b respectively.

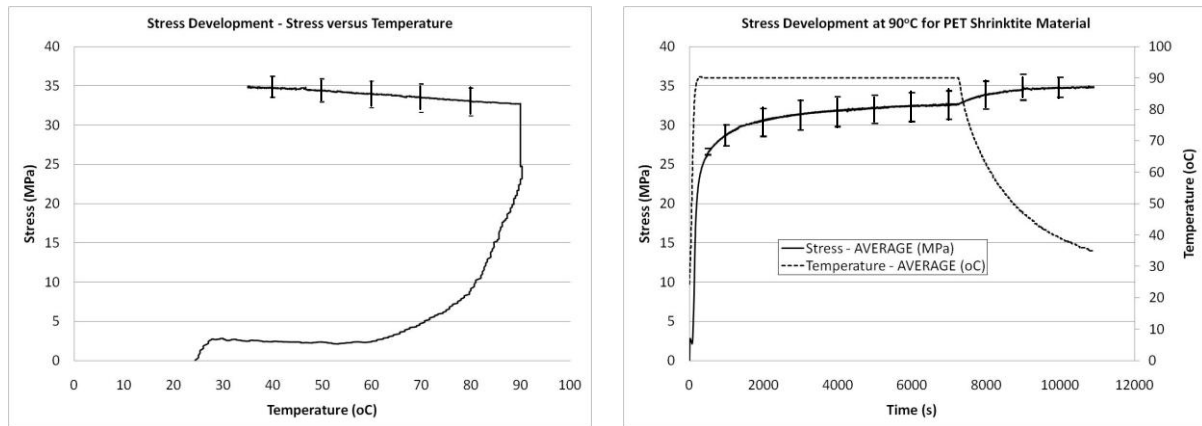


*Figure 3: Stress Development with (a) Temperature and (b) Time*

The results show that a shrinkage stress of 32.5MPa is achieved following the 3 hour soak at 90°C. The generation of this shrinkage stress is a known property of drawn shape memory polymers such as PET, whose molecules are stretched into a more random configuration during the drawing process. The effect of heating is to release these molecules which tend toward their favourable coiled conformation due to entropic considerations. In their restrained condition the molecules cannot retract and therefore generate a shrinkage force as the entropic forces balance with the external constraint. As the molecules enter a state of tension it is known that their ability for shrinkage is reduced and hence the stress plateau (27). The subsequent rise in stress following the return to ambient is the result of two effects: the thermal contraction of the steel equipment in the thermal chamber and the thermal contraction of the polymer. The thermal contraction of the polymer before and after the temperature soak can be seen to vary (slope of the stress-temperature graph) which is consistent with the observations of Bhushan (28) who proposed that the coefficient of thermal expansion increases slightly following annealing (heating above the transition temperature, 75°C).

### 3.2.3. Development of Young's Modulus with Temperature

The specimen was held at constant load while the temperature was raised in 10°C increments from 30°C to 160°C while the displacement, temperature and time were recorded. At each temperature increment the specimen was soaked for 5 minutes before increasing the load by 10N at a chosen rate, three rates were investigated: 10N/s, 1N/s and 0.1N/s. The load was then decreased by 10N at the chosen rate monitoring the stress, strain and time at a frequency of 100Hz during both the loading and unloading. The loading and unloading cycle is referred to as an "E-Value" test and is repeated at every temperature increment. A graph of Young's modulus with temperature can be seen in Figure 4.

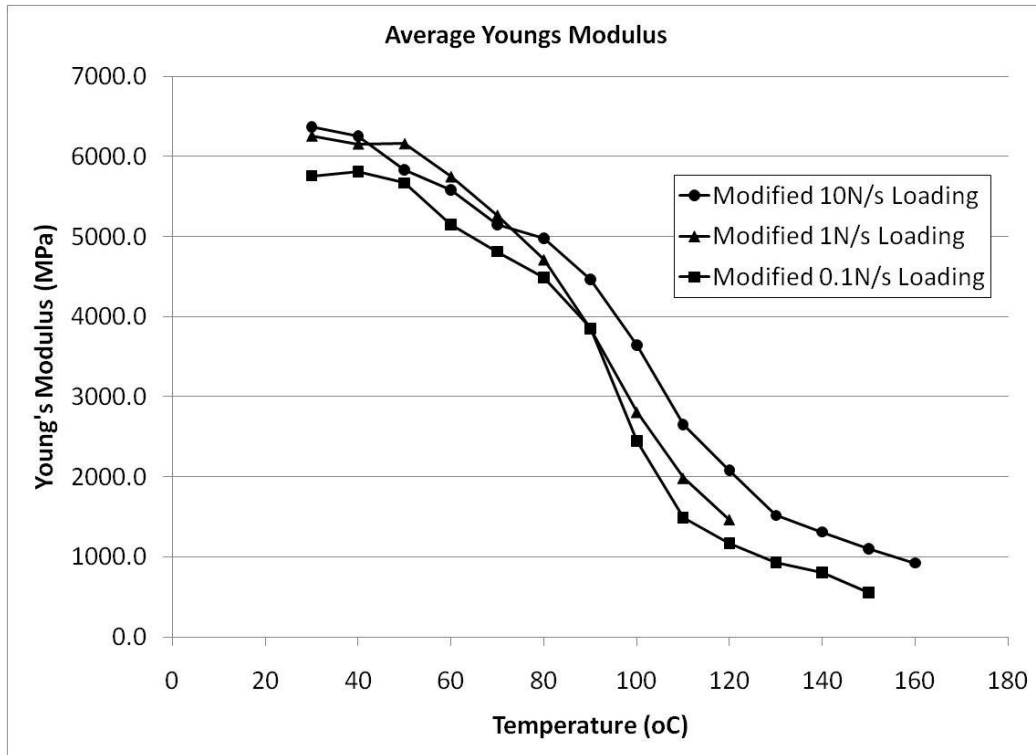


*Figure 4: Young's Modulus with Temperature*

The graphs show a clear relationship between the Young's modulus and temperature. Prior to 70°C (known as the glass transition temperature) the Young's modulus is constant at approximately 6000MPa. Following the glass transition temperature a transition of an exponential form was observed prior to the lower plateau of approximately 1000MPa at 120°C. These observations are consistent with those of Tobushi et al (29). The trend is the same for the different loading rates, however the faster loading rates have a slightly higher value throughout indicating that the Young's modulus is rate dependent to a certain degree.

### 3.2.4. Conclusions

The experimental studies have highlighted Aerovac Shrinktite, as a suitable polymer for the proposed system. The material generates a shrinkage stress of 32.5MPa at 90°C which is a suitable temperature and stress for applications involving concrete. Furthermore, a clear relationship between the Young's modulus and temperature has been found and will be required in the development of a numerical model for the polymer.

### 3.3. Numerical Simulation of Shape Memory Polymer

Existing numerical models for the simulation of temperature dependent shrinkage processes in PET were investigated in order to develop the subsequent numerical model. Pioneering work by Henry Eyring in the 1940s marked the start of such models and formulated that the deformation behaviour of polymers was a thermally activated rate process involving the motion of segments of chain molecules over potential barriers (30). Eyring proposed that a temperature dependant dashpot replace the existing dashpot in the Standard Linear Model. This model represents non-linear viscoelastic behaviour and is related to physical parameters in that it requires the input of an activation volume and activation energy.

Based on the principles proposed by Eyring, but taking a different approach was the work initially carried out by Trznadel (31) and progressed by Morshedean (32). They proposed a four-state model that qualitatively describes the temperature dependence of polymers. The model is characterized by two elastic springs and two two-site elements. It is the two-site elements that make the model unique and they are described as modelling the local properties of a molecular subunit and its interactions with the matrix. The two two-site elements have 4 possible configurations each relating to different conditions of deformation behaviour of the polymer.

Tobushi et al (33) proposed that the isothermal mechanical behaviour of polymers can be described by a four element rheological model consisting of an elastic spring and viscous dashpot in parallel with a friction element and another viscous dashpot. It is the friction element that models the effect of shape memory strain. Tobushi also proposed, in a later paper (29), that the material parameters (Modulus of elasticity, viscosity, retardation time and coefficient of thermal expansion) should be expressed by an exponential function of temperature.

The model on which Eyring is based; the basic Standard Linear Solid (SLS) model; is usually attributed to Zener (34). The SLS model consists of an elastic spring in parallel with a Maxwell unit (spring and dashpot in series) and gives a good approximation of observed behaviour of polymers in their viscoelastic range. The model describes both creep and stress relaxation in addition to the transition from a glassy (short term) modulus to the rubbery (long term) modulus. However this SLS model fails to include the effect of temperature and shrinkage on the deformation behaviour of polymers.

The proposed numerical model has been developed through consideration of the above mentioned existing models and the methods they employ along with the observations made in the experimental studies. The model aims to simulate the stress-strain-temperature-time behaviour of PET in a 1D uniaxial form.

### 3.3.1. Proposed Constitutive Model

A rheological representation of the proposed model can be seen in Figure 5 and consists of an elastic spring ( $E_1$ ) in parallel with a temperature dependant elastic spring ( $E_2$ ) and a temperature dependant viscous dashpot ( $\eta$ ).

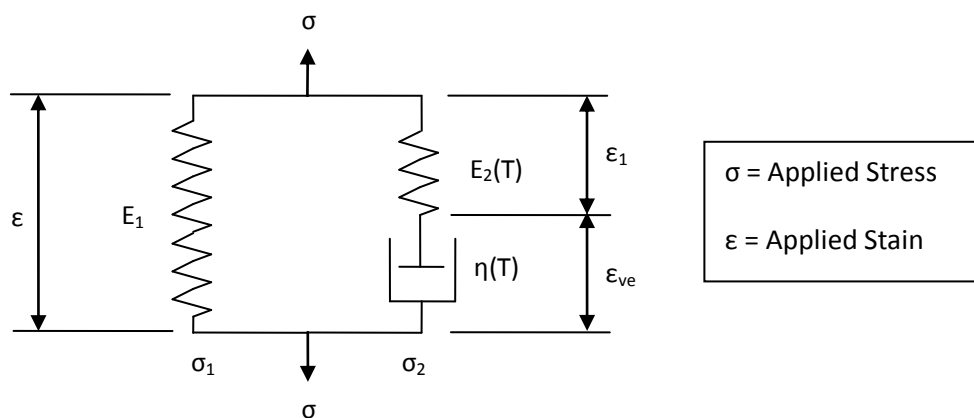


Figure 5: Rheological Representation of Proposed Model

The general stress conditions of the model are given by:

$$\sigma = \sigma_1 + \sigma_2 \quad [1]$$

$$\sigma_1 = E_1 \cdot \varepsilon \quad [2a]$$

$$\sigma_2 = E_2(T) \cdot \varepsilon_1 = \eta \cdot \dot{\varepsilon}_{ve} \quad [2b]$$

A time stepping process is used to obtain the solution of equations (1) and (2) in terms of the temperature dependant relaxation time ( $\tau_{func}$ ) and the previous viscous strain.

$$\varepsilon_{ve_j} = \varepsilon_{\theta_j} \left( 1 - e^{-\Delta t / \tau_{func}(T_{\theta_j})} \right) + \varepsilon_{ve_{j-1}} \cdot e^{-\Delta t / \tau_{func}(T_{\theta_j})} \quad [3]$$

An intermediate value of strain,  $\varepsilon_{\theta}$  is used and  $\theta$  is taken as 0.5. The current time step (j) is used along with the previous time step (j-1), while the temperature dependent relaxation time is given in equation (4):

$$\tau_{func}(T) = \frac{\eta(T)}{E_2(T)} \quad [4]$$

The temperature dependant viscosity is given by:

$$\eta(T) = \eta_H + (\eta_L - \eta_H) \cdot func_{\eta}(x(T)) \quad [5]$$

In which  $func_{\eta}(x) = \frac{e^{cx}}{(e^{cx} + f)}$  and  $x(T) = \frac{T - T_g}{T_H - T_L}$

The key temperatures used in the model are the current temperature (T), the temperature at the centre of the transition ( $T_g$ ) and the limiting temperatures  $T_H$  and  $T_L$  which can be seen in Figure 6 below. Figure 6 also highlights the values of  $E_1$  and  $E_{tot}$  which are experimentally derived from the 10N/s E-value tests. The constants b, c, d and f are fitting parameters.

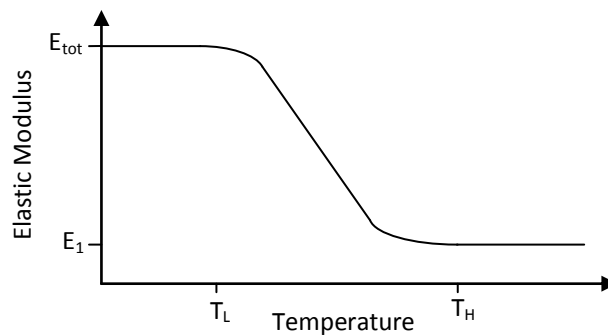


Figure 6: Idealised Young's Modulus with Temperature

Experimentally derived viscosities at the higher (i.e. melted) and lower (i.e. solid) temperatures are given by  $\eta_H$  and  $\eta_L$  respectively.

The elastic modulus,  $E_2$  is also temperature dependant where:

$$E_2(T) = E_{tot} + (E_1 - E_{tot}) \cdot func_{E_2}(\chi(T)) \quad [8]$$

$$func_{E_2}(x) = \frac{e^{bx}}{(e^{bx} + d)} \quad [9]$$

Equations (1), (2a) and (2b) are used to derive an equation for the stress in the system

$$\sigma_j = E_1[\varepsilon_j - \alpha_T(T_j - T_0)] + E_2(T) \cdot (\varepsilon_j - \varepsilon_{ve_j}) \quad [10]$$

Equation (10) highlights the constitutive behaviour for the polymer PET and also incorporates the coefficient of thermal expansion,  $\alpha_T$ . This takes into account the effect of thermal expansion on the total strain, which is significant prior to the onset of shrinkage. Investigations into the effect of shrinkage on the coefficient of thermal expansion are not considered here and are the subject of future work.

### 3.3.2. Comparison of Numerical and Experimental Material Properties

The following table details the input values that are used in the above proposed model.

Numerical Input Values			
Name	Symbol	Value	Unit
Ambient Temperature	$T_0$	30	$^{\circ}\text{C}$
Coefficient of Thermal Expansion	$\alpha_T$	$10^{-4.1}$	(-)
Young's Modulus at Low Temperature	$E_1$	925	MPa
Young's Modulus at High Temperature	$E_{tot}$	6373	MPa
Transition Start Temperature (Young's Modulus)	$T_L$	70	$^{\circ}\text{C}$
Transition End Temperature (Young's Modulus)	$T_H$	120	$^{\circ}\text{C}$
Temperature at Centre of Transition (Young's Modulus)	$T_g$	95	$^{\circ}\text{C}$
Fitting Constant	b	3.3	(-)
Fitting Constant	d	1.2	(-)
Stress at Drawing	$\sigma_{res}$	36	MPa
Viscosity at High Temperatures	$\eta_{2L}$	$1.575 \times 10^4$	Poise
Viscosity at Low Temperatures	$\eta_{2H}$	$4 \times 10^7$	Poise
Transition Start Temperature (Viscosity)	$T_L$	30	$^{\circ}\text{C}$
Transition End Temperature (Viscosity)	$T_H$	110	$^{\circ}\text{C}$
Temperature at Centre of Transition (Viscosity)	$T_g$	70	$^{\circ}\text{C}$
Fitting Constant	c	25	(-)
Fitting Constant	f	0.5	(-)

The faster loading rate results (10N/s) were used to determine values for the  $E_2$  component as the faster rate ensures that no viscous effects occur during the experiment and that the results are purely elastic. Figure 7(a) compares the experimentally derived results with the numerically derived results that are the produced using equation (8). The comparison shows a very good agreement.

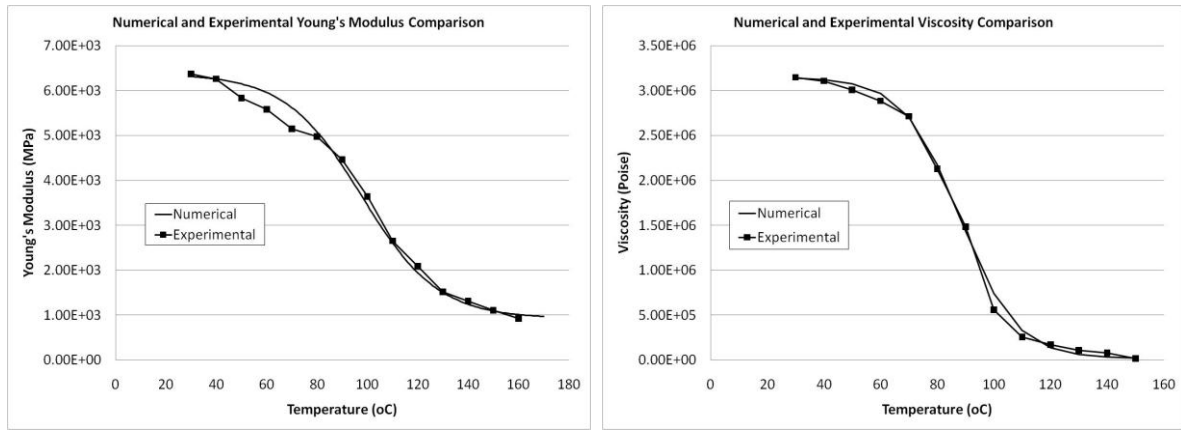


*Figure 7: Comparison of Numerical and Experimentally Derived Material Properties, (a) Young's Modulus and (b) Viscosity*

The viscosity variation with temperature is derived using a backward calculation from the slower and faster loading rate E-value tests. The slower rate will incorporate the viscous effects whereas the faster rate is purely elastic. An apparent Young's modulus is defined:

$$E_{app} = \frac{\Delta\sigma}{\Delta\varepsilon} \quad [11]$$

The change in viscous strain is then determined using equations (1) and (11) in which  $E_1$  and  $E_{tot}$  are defined in Figure 6,  $E_2$  values are taken from Figure 7a and  $E_{app}$  is the apparent Young's modulus determined from the slower (0.1N/s) loading rate which includes the viscous component:

$$\Delta\varepsilon_{ve} = \Delta\varepsilon \left( 1 - \frac{E_{app} - E_1}{E_2(T)} \right) \quad [12]$$

Equations (12) and (3) are then compared neglecting the array formulations in equation (3) and rearranged to yield for a time  $t=\Delta t$  the expression for the experimentally determined viscosity:

$$\eta = \frac{-\Delta t \cdot E_2}{\ln\left(\frac{E_{app} - E_1}{E_2(T)}\right)} \quad [13]$$

Figure 7(b) compares the experimentally derived viscosity with the viscosity derived numerically in equation (6) and show excellent agreement.

### 3.4. Comparison of Numerical and Experimental Data

A numerical simulation of the stress development with temperature experiments described previously was carried out using the material data given in the above table. A comparison of the numerical and experimental results can be seen in Figure 8 and show excellent agreement.

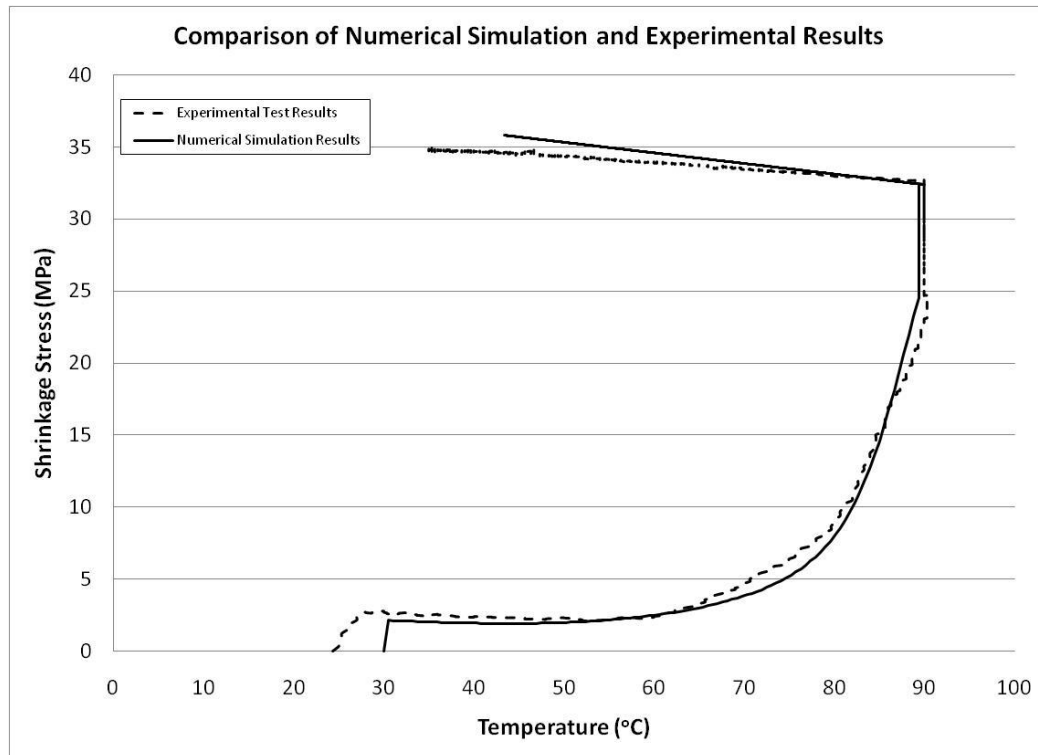


Figure 8: Comparison of Experimental and Numerically Derived Results

## 4. Conclusion and Future Work

A series of experimental studies have been presented which highlight Aerovac Shrinktite PET as a suitable polymer for the proposed self healing concrete system. The PET generates a shrinkage stress of 32.5MPa which far surpasses the required 20MPa. The stress is also achieved at a suitable temperature of 90°C.

Further experimental studies have provided detailed information on the material behaviour of the PET. The Young's modulus has been found to follow a clear exponential trend between the limits of 70°C and 120°C at which points the Young's Modulus is constant at approximately 6000MPa and 1000MPa respectively.

A successful numerical model has been proposed which accurately simulates the shrinkage behaviour of PET. The proposed numerical model can now be confidently used in conjunction with a concrete material model to simulate the entire system. This simulation will be compared to the experimental work undertaken on the combined system and also used to predict effects which cannot be easily carried out in the laboratories. A further 3D development of the polymer numerical model will also enable a full 3D analysis of the system to be undertaken.

## Acknowledgements

The author would like to acknowledge Prof. Lark, Dr Jefferson, Dr Joseph and Ben Isaacs of Cardiff University for their participation in the development of the new cementitious-shape memory polymer composite.

## Bibliography

1. Energy efficient cement could radically cut emissions. *www.energyefficiencynews.com*. [Online] [Cited: 20 December 2009.] <http://www.energyefficiencynews.com/i/1665/>.
2. **Worrell, E, et al.** 2001, Annual Review of Energy and Environment, 2001, Vol. 26.
3. **IATA.** 2009, Aviation Environment. *www.iata.org*. [Online] [Cited: 20 December 2009.] [http://www.iata.org/whatwedo/environment/climate\\_change.htm](http://www.iata.org/whatwedo/environment/climate_change.htm).
4. **DTI.** 2006, *Construction statistics annual report 2006*. London : TSO.
5. *Eurocode 2: Design of concrete structures - Part 1-1: General rules and rules for buildings. EN1992-1-1.* 2004.
6. **Lark, R L, et al.** 2010, Cement and Concrete Research, Accepted January 2010
7. **RILEM.** 2009, *STAR - Self Healing Materials (DRAFT)*. : RILEM.
8. **Schlangen, E.** 2005, Self-healing phenomena in cement-based materials. *RILEM*. [Online] [http://www.rilem.org/tc\\_shc.php](http://www.rilem.org/tc_shc.php).
9. **van Tittelboom, K and De Belie, N.** 2009, 2nd International Conference on Self Healing Materials, Chicago.
10. **Joseph, C.** 2008, *Experimental and Numerical Study of the Fracture and Self-Healing of Cementitious Materials - PhD Thesis*. : Cardiff University.
11. **Reinhardt, H-W and Loos, M.** 2003, Cement and Concrete Research 33, pp. 981-985.
12. **Zhong, S and Yao, W.** 2008, Construction and Building Materials 22(6), pp. 1137-1142.
13. **Jacobsen, S and Sellevold, E J.** 1996, Cement and Concrete Research, 26(1), pp. 55-62.
14. **Edvardsen, C.** 1999, ACI Materials Journal, 96(4), pp. 448-454.
15. **Ter Heide, N, Schlangen, E and van Breugel, K.** 2005, Knud Hoejgaard Conference on Advanced Cement-Based Materials, Technical University of Denmark
16. **Dry, C M.** 1994, Smart Materials and Structures, 3(2), pp. 118-123.
17. **Nishiwaki, T, et al.** 2006, Journal of Advanced Concrete Technology, 4(2), pp. 267-275.
18. **Mihashi, H, et al.** 2000, Transactions of the Japan Cement Institute 22, pp. 441-450.
19. **Li, V C, Yun Mook, L and Yin-Wen, C.** 1998, Composites Part B: Engineering, 29(6), pp. 819-827.

20. **Jonkers, H M and Schlangen, E.** 2009, 2nd International Conference on Self-healing Materials, Chicago.
21. **Lark, R L, et al.** 2009, Cement and Concrete Research, (Submitted).
22. **Jefferson, A D, Lark, R L and Joseph, C.** 2007, *GB0715123* Great Britain/Wales.
23. **Dunn, S C, et al.** 2009, 2nd International Conference for Self-healing Materials, Chicago.
24. **Isaacs, B, et al.** 2010, Cement and Concrete Research, (In Progress).
25. **Lark, R J, et al.** 2009, 2nd International Conference of Self-Healing Materials, Chicago.
26. **Dunn, S C, et al.** 2010, Polymer (Submitted).
27. **Gupta, V B, Radhakrishnan, J and Sett, S K.** 1994, Polymer 12, Vol. 35.
28. **Bhushan, Bharat.** 2000, *Mechanics and reliability of flexible magnetic media - 2nd Edition.* New York : Springer-Verlag.
29. **Tobushi, H, et al.** 2001, Mech. Mat. 33, p. 545.
30. **Halsey, G, White, H J and Eyring, H.** 1945, Textiles Research Journal 15, p. 295.
31. **Pakula, T and Trznadel, M.** 1985, Polymer 26, p. 1011.
32. **Morshedian, J, Khonakdar, H A and Rasouli, S.** 2005, Macromol Theory Simul 14 , p. 428.
33. **Bhattacharyya, A and Tobushi, H.** 2000, Poly. Engin. Sci. 40, p. 2498.
34. **Zener, C.** 1948, *Elasticity and Anelasticity of Metals.* Chicago : Chicago University Press.